Biogeosciences Discuss., 7, 7821–7848, 2010
www.biogeosciences-discuss.net/7/7821/2010/
doi:10.5194/bgd-7-7821-2010

Biogeosciences Discussions

Production and consumption mechanisms of N_2O in the Southern Ocean revealed from its isotopomer ratios

N. Boontanon[1,2], S. Watanabe[3], T. Odate[4], and N. Yoshida[2,5]

[1]Faculty of Environment and Resource Studies, Mahidol University, 999 Phuttamonthon 4 Rd., Salaya, Phuttamonthon, Nakhon Pathom, 73170, Thailand
[2]SORST project, Japan Science and Technology Agency, 4-1-8 Honcho, Kawaguchi-shi, Saitama, 332-0012, Japan
[3]Japan Marine Science and Technology Center, 2-15 Natsushima-Cho, Yokosuka, Kanagawa, 237-0061, Japan
[4]National Institute of Polar Research, Kaga 1-chome, Itabashi-ku, Tokyo, 173-8515, Japan
[5]Department of Environmental Science and Technology, Interdisciplinary Graduate School of Science and Engineering, Tokyo Institute of Technology, 4259 Nagatsuta, Midori-ku, Yokohama, 226-8502, Japan

Received: 6 October 2010 – Accepted: 11 October 2010 – Published: 27 October 2010

Correspondence to: N. Boontanon (ennbt@mahidol.ac.th)

Published by Copernicus Publications on behalf of the European Geosciences Union.

Abstract

The distribution of dissolved N_2O in the Southern Ocean at 140° E was measured during the austral summer (February–March 2002) in the framework of the 43rd Japanese Antarctic Research Expedition (JARE-43). Surface-dissolved N_2O was undersaturated (about 94% saturation), and the calculated mean sea-air flux rate was $-3.68 \pm 2.57\ \mu mol\ m^{-2}\ d^{-1}$. The vertical distributions tested exhibited N_2O maxima at around 150–300 m (ΔN_2O, 7.90–8.51 nM) below the chlorophyll-rich layer, which coincided with the layer of minimum oxygen. These observations strongly suggest that N_2O production and consumption are related to apparent oxygen utilization (AOU). In the deeper layer, the presence of anoxic microsites within particles, together with the horizontal and vertical movement of cold water around Antarctica, is one of the parameters that govern the intramolecular distribution of the isotopic composition of N_2O. The N_2O isotopic compositions in the maximum layer were +7.3 to +8.2‰ for $\delta^{15}N_{bulk}$ and +43.5 to +46.2‰ for $\delta^{18}O$ associated with the coupling of nitrification and denitrification production mechanisms. Site preference decreased from an average 17‰ at the surface to the ΔN_2O maximum and slightly increased with depth up to 24‰ at the deeper region. The influence of deep Southern Ocean N_2O on the global N_2O budget is estimated to be about 46.2 ± 5.3 Mg N_2O-N d^{-1}, which represents the amount that can escape to the atmosphere and thus contribute to emissions into the world's oceans.

1 Introduction

Recently, considerable attention has been focused on the emission of biogenic trace gases from ecosystems, since they contain a significant amount of greenhouse gases, such as carbon dioxide, methane, and nitrous oxide. Nitrous oxide (N_2O) is a very effective heat-trapping gas in the atmosphere because it absorbs outgoing radiant heat in infrared wavelengths that are not captured by the other major greenhouse gases,

BGD
7, 7821–7848, 2010

such as water vapor and CO_2. By absorbing and reradiating this heat back toward the Earth, N_2O contributes only slightly (5–6%) to overall greenhouse warming (Bouwman, 1990). However, it plays a significant role in the destruction of the ozone layer in the stratosphere (Crutzen, 1970). The annual input of N_2O into the atmosphere is estimated to be ~14 Tg N_2O-N yr^{-1}, and the oceans are believed to contribute more than 17% of the total annual input (Watson et al., 1992). Thus, measurement of the N_2O budget at a global level may provide important information on greenhouse gas effects.

As a major component of the world's oceans, the Southern Ocean has several unique characteristics, including the circumpolar homogeneous nature of its physical and chemical variables, the immense expanse of cold surface water, and the pronounced seasonal variation at the surface compared to other ocean basins (Lutjeharms, 1990). N_2O is produced by the biological processes of nitrification and denitrification (Dore et al., 1998; Knowles et al., 1981; Rysgaard et al., 1993; Svensson, 1998; Ueda et al., 1993). Depending on the redox conditions, N_2O is produced from inorganic nitrogenous compounds (NH_3 or NO_3^-), with subsequently different isotopic fractionation factors. The isotopic signatures of N_2O confer constraints on the relative source strength, and the reaction dynamics of N_2O biological production pathways are currently under investigation. Furthermore, isotopomers of N_2O contain more easily interpretable biogeochemical information as to their sources than obtained from conventional bulk ^{15}N and ^{18}O measurements (Yoshida and Toyoda, 2000). Here, we describe the results of the first isotopomer studies of dissolved N_2O in the Southern Ocean, one of the most productive seas in the world, in order to examine the origins of N_2O in sea water and to estimate the inventory of N_2O with respect to the atmosphere.

BGD
7, 7821–7848, 2010

2 Materials and methods

2.1 Study sites and samplings

Samples were collected in the framework of the 43rd Japanese Antarctic Research Expedition (JARE-43) during the 2002 Marine Science Cruise on the R/V *Tangaroa* from 6 February to 7 March 2002. The purpose of the expedition was to study the biogeochemical cycles and biological processes of the Southern Ocean and their roles in the global environment. The production and consumption of dissolved N_2O in Southern Ocean ecosystems was investigated by collecting seawater samples at stations 1 (open water), 5 (marginal ice zone), and 8 (previous ice zone; Fig. 1). Water samplings were carried out at the indicated depths using a CTD water sampler (SBE 32 24 × 10-L Carousel Water Sampler). For N_2O analyses, water samples were introduced into 225-ml glass vial and then sterilized with mercuric chloride (1 ml saturated $HgCl_2$ solution per vial). The vial was then sealed with a butyl-rubber septum and an aluminum cap, taking care to avoid bubble formation, and then brought back to the laboratory and stored at 4 °C until the analyses were conducted.

2.2 Chemical analysis

Salinity and temperature were recorded using a CTD (SBE 911plus). Dissolved oxygen was measured with a dissolved oxygen auto-titrator on-board (based on the design of the Scripps Institution of Oceanography).

2.3 Dissolved N_2O and isotopomer analyses

At present, the analysis of very low concentrations of dissolved N_2O is difficult. The best way is to extract the N_2O in the sample using pure helium gas (He, 99.9999%) and then to concentrate it. Therefore, each water sample was transferred to a stripping chamber, and He was bubbled to extract the dissolved gases. H_2O and CO_2 were removed by passing the gases sample through a magnesium perchlorate ($Mg(ClO_4)_2$)

BGD
7, 7821–7848, 2010

and ascarite (sodium-hydroxide-coated silica) column, respectively. N_2O was then collected in a U-shaped tube filled with glass beads under liquid nitrogen. At the end of the quantitative extraction of N_2O, the U-tube was heated in a hot-water bath. The desorbed gas was introduced into a PreCon Unit under a helium flow. Sample gas was passed through a chemical trap to remove H_2O and CO_2. After the H_2O and CO_2 were removed, N_2O was cryo-focused in a U-trap at liquid nitrogen temperature. After removing the Dewar flask containing liquid nitrogen from the U-trap, the sample was separated on a PoraPlot Q column (25 m) at 27 °C, CO_2 and N_2O were separated by chromatography and the isotope ratios of N_2O was recorded with a mass spectrometer (Finnigan, MAT 252) using modified Faraday cups as the helium carrier flow. Isotopomer ratios of $\delta^{15}N^{bulk}$, $\delta^{15}N^{\alpha}$ (central nitrogen), $\delta^{15}N^{\beta}$ (terminal nitrogen), and $\delta^{18}O$ were obtained from mass analysis of N_2O^+ and fragment NO^+ formed in an ion source (Toyoda and Yoshida, 1999):

$$\delta X\,(‰) = [(R_{SAMPLE}/R_{STANDARD}) - 1] \times 1000$$

where X is $^{15}N^{bulk}$, $^{15}N^{\alpha}$, $^{15}N^{\beta}$, or ^{18}O of N_2O and $^{15}R^{bulk} = (^{15}R^{\alpha} + ^{15}R^{\beta})/2$, $^{15}R^{\alpha} = [^{14}N^{15}N^{16}O]/[^{14}N^{14}N^{16}O]$, $^{15}R^{\beta} = [^{15}N^{14}N^{16}O]/[^{14}N^{14}N^{16}O]$, $^{18}R = [^{14}N^{14}N^{18}O]/[^{14}N^{14}N^{16}O]$. Nitrogen and oxygen isotope ratios of dissolved N_2O are expressed in ‰ deviations from atmospheric N_2 and the Vienna standard mean ocean water (VSMOW), respectively. The reproducibilities of $\delta^{15}N^{\alpha}$, $\delta^{15}N^{\beta}$, $\delta^{15}N^{bulk}$, and $\delta^{18}O$ were ±0.9‰, ±1.5‰, ±0.6‰, and ±0.9‰, respectively. The atmospheric equilibrium concentration of N_2O was calculated from the in-situ water temperature and the atmospheric mixing ratio (310 ppbv) following the methods of Weiss and Price (1980).

BGD
7, 7821–7848, 2010

3 Results

3.1 Vertical distributions of dissolved N_2O and its isotopomers

The N_2O concentration profile at stations 1 and 5 were similar to those observed in the open ocean (Toyoda et al., 2002; Yoshida et al., 1989) and correlated strongly with apparent oxygen utilization (AOU; Figs. 3–6). Everywhere at the surface, N_2O concentrations were lower than those at atmospheric equilibrium. Excess N_2O (ΔN_2O) increased significantly toward the continental margins, with a mean ΔN_2O of −0.88 nM (93.9%). The isotopic compositions of dissolved N_2O were also slightly enriched in the same direction, from 8.1 to 8.5‰ for $\delta^{15}N_{AIR}$ and 45.6 to 46.5‰ for $\delta^{18}O_{VSMOW}$. The isotopomers varied more than the bulk $\delta^{15}N$, the site preference ($\delta^{15}N^{\alpha} - \delta^{15}N^{\beta}$) value of 18.4‰ at station 1 was nearly the same as that of N_2O in the troposphere (Yoshida and Toyoda, 2000). About 3‰ depletion was observed at the shallower region (station 8).

The vertical distribution of dissolved N_2O consisted of supersaturation at the subsurface and throughout the water column (Figs. 3–5). The N_2O depth profiles showed a concentration maximum between 100 and 200 m. The ΔN_2O maximum (7.90–8.51 nM) was observed in the oxygen minimum layer, similar to results reported in the literature (e.g., Naqvi et al., 1994; Toyoda et al., 2002; Yoshinari, 1976). The ΔN_2O concentration generally decreased below 200 m at both stations 1 and 5. At station 8, the profile did not show a N_2O maximum at the subsurface, but the ΔN_2O concentration became supersaturated near the bottom. Bulk nitrogen and oxygen isotope ratios of dissolved N_2O at stations 1 and 5 showed a subsurface minimum at the ΔN_2O maximum layer while both $\delta^{15}N^{bulk}$ and $\delta^{18}O$ maxima were measured at the bottom, with a slight increase with depth. At station 8, the values of both $\delta^{15}N^{bulk}$ and $\delta^{18}O$ were constant throughout the water column. Isotopomers of nitrogen, especially with respect to site preference, showed some vertical variation from the subsurface to the deeper layers. Site preference decreased at the ΔN_2O maximum and slightly increased with depth. A

BGD
7, 7821–7848, 2010

site-preference maximum peak at station 1 was detected at a depth of about 2200 m and then decreased towards the bottom. At station 5, a site-preference maximum was found at about 2000 m and at the bottom. At station 8, the ΔN_2O and isotopic compositions did not change, while site preference fluctuated greatly throughout the water column. Site preference maxima were detected at a depth of 60–140 m and also at the bottom.

4 Discussion

4.1 Surface N_2O and the kinetic equilibrium

Dissolved N_2O in the surface layers of the sea is usually at or near saturation, while the N_2O concentrations in the Southern Ocean surface layer were found to be below atmospheric equilibrium; however, this is not surprising, as a similar phenomenon was also observed in another ocean (Naqvi et al., 1994). Several processes control N_2O concentration in the surface water, and physical factors, mainly temperature and wind, normally affect gas saturation values up to about 5% above or below saturation (Bieri et al., 1966, 1968). The decrease in the surface equilibrium of N_2O in the Southern Ocean may be associated with an increase in the transfer velocity, which is mainly related to wind speed since the temperature around this area is quite stable during February and March. In the Antarctic, the ocean area from about latitude 40° S to the Antarctic Circle has the strongest winds speeds recorded anywhere on Earth (CIA, 2003). Broecker and Siems (1994) reported that when wind speed exceeds 10 m s^{-1}, waves begin to break, causing the formation of air bubbles that become entrained in the water. This, in turn, results in gas exchange at the surface layer between the air bubbles and seawater. During our study, the average wind speed in the area of the sampling sites increased and ranged from 6.8 m s^{-1} at station 8 to 10.6 m s^{-1} at station 1. Therefore, these data support the finding of a decrease in the surface equilibrium (from −0.62 to −1.32 nM).

BGD
7, 7821–7848, 2010

In the surface water, the isotopic composition of dissolved N_2O is governed by gas exchange with atmospheric N_2O. Inoue and Mook (1994) reported that the kinetic fractionation factors for dissolved N_2O during N_2O invasion and evasion are slightly greater (about 0.7‰ for $\delta^{15}N$ and 1.1‰ for $\delta^{18}O$) than those in air. The kinetic fractionation factors of $\delta^{15}N$ and $\delta^{18}O$ being transferred across the interface can be calculated using the following equations:

$$\alpha_{inv} = R_{inv}/R_g = k^i_{inv}/k^j_{inv} \quad (1)$$

and

$$\alpha_{ev} = R_{ev}/R_l = k^i_{ev}/k^j_{ev}, \quad (2)$$

where R_{inv} and R_{ev} refer to the isotopic compositions of the invading and evading N_2O, respectively; R_g and R_l refer to the isotopic compositions of gaseous and dissolved N_2O; k_{inv} represents the transfer coefficient for the invasion process; k_{ev} represents the transfer coefficient for the evasion process; and superscript i is an isotope heavier than j. The equilibrium fractionation factor α between the gas and water phases is related to the kinetic factors by considering the fact that at equilibrium, R_{inv} must be equal to R_{ev}.

$$\alpha_{ev}/\alpha_{inv} = (R_{ev}/R_l)/(R_{inv}/R_g) = R_g/R_l = \alpha \quad (3)$$

Nitrogen (bulk) and oxygen isotope ratios of dissolved N_2O are about 1‰ higher in the surface water of the Southern Ocean than in the troposphere, 7.0 and 44.7‰ for $\delta^{15}N$ and $\delta^{18}O$, respectively (Kim and Craig, 1993), which agrees with the equilibrium isotope fractionation. However, oxygen isotopes of surface-water N_2O are more fractionated than nitrogen isotopes. Significant kinetic fractionation of oxygen isotopes during gas transfer at water surfaces seems to be related to short-range interactions with the oxygen atom in N_2O, which makes the lighter molecule more soluble at the transition state; this is similar to the results of Inoue and Mook (1994). Furthermore, compared to the isotope compositions of dissolved N_2O at the other stations, those at

BGD
7, 7821–7848, 2010

station 1, where a higher wind speed was expected to cause a higher N_2O exchange rate between surface water and air, were closer to those of the troposphere. Thus, the exchange of N_2O between ocean and atmosphere and its isotopic fractionation should be treated kinetically and varies with time and space.

Similar to the isotopic compositions of N_2O, a site preference of about 17.0‰ on average was observed, in that ^{15}N at the center (α-center) was enriched compared with the end-site nitrogen (β-site). This value is close to that measured in the troposphere (Yoshida and Toyoda, 2000). However, the site preference was depleted between station 1 and station 8 due to the enrichment of $\delta^{15}N^{\beta}$, while the difference was smaller for $\delta^{15}N^{\alpha}$, which suggests that the heavier isotope of the β-site nitrogen ($^{15}N^{14}N^{16}O$) is slightly more soluble in water compared to $^{14}N^{14}N^{16}O$. The former was caused by the significant difference in solute-solvent interaction (dispersion) energies between lighter and heavier molecules. The equilibrium fractionation of $\delta^{15}N^{\beta}$ in the Southern Ocean ranged from +1.8 to +3.8‰ relative to tropospheric $\delta^{15}N^{\beta}$-N_2O (~ –3‰; Yoshida and Toyoda, 2000), and the fractionation is much larger than that of $\delta^{15}N^{bulk}$ (+1.1 to +1.5‰). This may be a result of the kinetic fractionation of the β-site nitrogen, which is much more active than the center nitrogen during gas transfer across the gas-liquid interface. During invasion, two processes have to be considered: dissolution and molecular diffusion near the surface, whereas during evasion there is only molecular diffusion from the water mass to the surface (Inoue and Mook, 1994).

4.2 Production and consumption of N_2O in the water column

In the ocean, AOU reflects the amounts of O_2 consumed by respiration and nitrification in water since its last contact with the atmospheric O_2 at the surface. The correlation between ΔN_2O and AOU provides circumstantial evidence that nitrification is the dominant mechanism of N_2O production (Butler et al., 1989; Cohen and Gordon, 1979; Elkins et al., 1978; Yoshinari, 1976). At below mixed layer to N_2O maximum layer, O_2 is consumed in the process of nitrification whereby nitrate is regenerated. The correlation

BGD
7, 7821–7848, 2010

gradient between ΔN_2O and AOU at the productive layer (Fig. 6) is closed to that reported by Cohen and Gordon (1979) in the Northwestern Atlantic and Northwestern Pacific suggested that N_2O production in the ocean primarily arises from nitrification (Cohen and Gordon, 1978; Yoshinari, 1973). While the generally flat relationship between ΔN_2O and AOU below the productive layer may due to the denitrification takes place whereby O_2 are not utilized by this process. However, the coincidence with the isotopic studies of dissolved N_2O much more clearly understands the reaction dynamics of N_2O biological pathways.

The N_2O maxima observed at the subsurface (150–300 m) of the Southern Ocean were produced by the decomposition of sinking particles during the summer season. In the waters of the Southern Ocean surrounding Antarctica, a phytoplankton bloom fueled by nutrient-rich waters leads to the growth of vast swarms of krill (*Euphausia superba*) each summer. Consequently, settling particles, such as fecal pellets, may be produced during the life cycle of the krill, either directly or indirectly. Chlorophyll-*a* is the most important among several kinds of phytopigments and can be used as a semi-quantitative measurement of phytoplankton abundance. Hirawake et al. (2003) reported that the chlorophyll-*a* concentration clearly shows a seasonal variation, with a complicated spatial distribution. The chlorophyll-*a* concentration was very low ($<0.3\,mg\,m^{-3}$) in October, but rapidly increased up to $1–5\,mg\,m^{-3}$ through December near the sea-ice edge and in the open ocean.

The N_2O isotopic compositions in the maximum layer, +7.3 to +8.2‰ for $\delta^{15}N_{bulk}$ and +43.5 to +46.2‰ for $\delta^{18}O$, were similar to the values measured in other oceans (Kim and Craig, 1993; Naqvi et al., 1998) and freshwater ecosystems (Boontanon et al., 2000; Ueda et al., 1999). As reported in several aquatic systems, dissolved N_2O can be categorized into three types according to the intramolecular distributions of $\delta^{15}N_{AIR}$ and $\delta^{18}O_{VSMOW}$ in N_2O: oxic, anoxic, and semi-anaerobic N_2O (Boontanon et al., 2000). Under oxic conditions, by-product N_2O, produced during nitrification (Yoshida and Alexander, 1970), accumulates with no further oxidation or reduction. Yoshida (1988) reported very low $\delta^{15}N^{bulk}$, from −60 to −68‰, for N_2O produced

BGD
7, 7821–7848, 2010

during ammonium oxidation in pure cultures of *Nitrosomonas europaea*, while the oxygen atom of N_2O produced via nitrification is derived from both O_2 and H_2O in ambient water (Ostrom et al., 2000; Schmidt and Voerkelius, 1989). Under anoxic conditions, intermediate N_2O is enriched in ^{15}N and ^{18}O compared with oxic N_2O. Wahlen and Yoshinari (1985) reported this type of N_2O in Green Lake. Semi-anaerobic N_2O, produced during the simultaneous occurrence of oxidation-reduction processes, represents a coupling between the other two processes and may be an important mechanism of N_2O production (Boontanon et al., 2000; Naqvi et al., 1998). In the Southern Ocean, the isotope ratios of N_2O suggest that N_2O is produced by the simultaneous occurrence of nitrification and denitrification processes taking place in the sinking particles (Alldredge and Cohen, 1987). With respect to the occurrence of redox conditions within an organic particle, Alldredge and Cohen (1987) and Kaplan and Wofsy (1985) suggested that denitrification occurred, even in oxygenated water, as long as the large diameter of the particulate organic matter could provide anaerobic conditions in the center of the particle. N_2O produced during nitrification in the outer oxic layer could diffuse into the inner layer and partly be incorporated into denitrification processes. This kind of multi-occurrence of oxidation-reduction could explain the different isotopic signatures of N_2O. In addition, when N_2O was produced via denitrification, $\delta^{15}N^{bulk}(N_2O)$ values increased nearly to that of $\delta^{15}N(NO_3^-)$ (5–7‰; Sigman et al., 1999; Wada et al., 1987). Ostrom et al. (2000) reported the enrichment of ^{18}O by approximately 20‰ during nitrification, since the $\delta^{18}O$ of dissolved O_2 was significantly high (+24.7‰), and N_2O produced by nitrification was enriched in ^{18}O by +43 to +46‰ relative to seawater $\delta^{18}O$.

Since site preference should mainly depend on production or consumption mechanisms, analysis of the isotopomers of N_2O should distinguish the production mechanism of the N_2O under investigation. In the above, the proposed N_2O production mechanism can be explained by the coupling of nitrification and denitrification. Isotopic fractionation governed by kinetic isotope effects occur during the reaction sequences $NH_4^+ \rightarrow NO_2^- \rightarrow NO \rightarrow N_2O$ for the outer layer, while the oxidation of NOH does not

BGD
7, 7821–7848, 2010

involve a primary kinetic isotope effect and thus should not markedly affect site preference (Popp et al., 2002). In N_2O generated by dissimilatory nitrite reduction (Weeg-Aerssens et al., 1988), the N-N bond of N_2O is formed by a nucleophilic attack of a second nitrite on a metal-coordinated nitrosyl species (Fig. 7). The first N ultimately occupies the β-position, and fractionation could result in nitrite binding to the ferrous heme following by nucleophilic attack of NO_2^- on the coordinated nitrosyl species, resulting in the formation of the N-N bond. While this reaction sequence may also allow isotope discrimination, exchange of the two nitrogens in the intermediate may also occur during N_2O formation, resulting in a more complicated isotopic fractionation of N_2O isotopomers. Furthermore, the reaction may cause depletion of ^{15}N both in the center and in the terminal nitrogen of N_2O, because as the reaction approaches completion, the isotopic composition of the product approaches that of the initial substrate. Thus, N_2O released during the initial phase by the decomposition of sinking particles, at a depth of 60–200 m at station 1 and 60–100 m at station 5, will be depleted in ^{15}N at both N^{α} and N^{β} sites when the level of nitrification is greater than the level of denitrification. Due to the utilization of substrate nitrogen, $\delta^{15}N$ values of the substrate are enriched and result in a small enrichment of ^{15}N at both N^{α} and N^{β} sites at the N_2O maximum layer (300 m at station 1 and 150 m at station 5). Below the N_2O maximum layer, the inner layer becomes anaerobic and denitrification can take place using the accumulated NO_3^-. Consequently, N_2O quickly decreases because of its reduction to N_2. Following cleavage of the N-O bond of N_2O during denitrification, associated isotopic fractionation should show enrichment of both ^{15}N at the N^{α} position and of $\delta^{15}N^{bulk}$ and $\delta^{18}O$.

In the deeper layer, below 500 m, at steady state, denitrification takes place in anoxic microsites within particles that could also serve as sites of active reduction of N_2O to N_2. This, in turn, preferentially removes the lighter isotope thereby successively enriching the remaining unreacted N_2O in ^{15}N and ^{18}O. Thus, partly escaped N_2O is slightly enriched in $\delta^{15}N^{bulk}$, $\delta^{18}O$, and $\delta^{15}N^{\alpha}$ while there is only a small fluctuation in $\delta^{15}N^{\beta}$. During denitrification, $\delta^{15}N$ and $\delta^{18}O$ of produced N_2O are expected to be

BGD
7, 7821–7848, 2010

either similar or more enriched than $\delta^{15}N$ and $\delta^{18}O$ of the substrate NO_3^- (Wada et al., 1996). However, N_2O was found to be more enriched in ^{15}N and ^{18}O compared to NO_3^- ($\delta^{15}N$ of NO_3^- from Sigman et al., 1999) in the deeper layers at both stations 1 and 5, which is similar to what was found in the western North Pacific (Yoshida et al., 1989). This indicates that most of the N_2O is involved in NO_3^- reduction. N_2O is both consumed and produced during NO_3^- reduction. As a result, the $\delta^{15}N$ and $\delta^{18}O$ of N_2O are determined by the fractionation factors during production and consumption. Yoshida (1984) reported a kinetic nitrogen isotope fractionation factor for the reduction of N_2O by denitrifying bacteria of up to 1.028 in terms of the rate-constant ratio of the isotope species. If the ^{15}N and ^{18}O enrichment of the substrates is greater during consumption than during production, enrichment in both ^{15}N and ^{18}O of N_2O relative to NO_3^- should result. Furthermore, in deep water, horizontal and vertical movements of cold water from close to shore, induced by the geopotential anomaly of the strong steering current of the ridge system around the Antarctic (see Lutjeharms, 1990; Orsi et al., 1995), should be one of the parameters controlling the isotopic composition of N_2O (Fig. 8).

It should be noted that at station 8, which is a shallow water column close to the shore, the strong steering current in the summer may promote homogeneity of both the N_2O concentration and the isotopic composition from the surface to the bottom. To clearly understand the variability in the isotopomers of N_2O, culture studies are needed in which media composition, substrate concentrations, and rates of the reactions are well regulated.

4.3 Sea-to-air flux and N_2O budget in the Southern Ocean

The degassing of surface sea water could release N_2O into the atmosphere by simple diffusion and contributions to the net flux of N_2O across the sea-air interface. Based on our data, it is premature to quantitatively calculate the influence of the Southern Ocean on the global N_2O budget; however, several insights can be pointed out. The estimated

BGD
7, 7821–7848, 2010

value of N_2O that will eventually reach the atmosphere after transport through the unsaturated zone can be determined from the empirical relationship between wind speed and gas transfer, using measured values of wind speed, temperature, and the surface concentration of N_2O, according to the following equation (Liss and Slater, 1974):

$$F = K_L(C_S - C_E) \quad (4)$$

where K_L is the liquid-phase gas-transfer coefficient, C_S is the gas concentration in the surface water; and C_E is the gas concentration of the solution during equilibrium with the overlying gas phase.

By using the average wind speed measured during the sampling period, the N_2O sea-air flux was −1.45 (St. 8) to −6.50 (St. 1) μmol m^{-2} d^{-1}, with an average of −3.68 ± 2.57 μmol m^{-2} d^{-1}. A negative flux value has also been observed in the Bay of Bengal (−0.10 μmol m^{-2} d^{-1}; Naqvi et al., 1994). In the Antarctic Zone, mixing is greatest in the summertime T_{min} layer. During the austral summer, the summer surface mixed layer is underlain by a roughly 200-m-thick minimum temperature layer (the T_{min} layer), and the deep portion of the winter mixed layer becomes isolated from the surface due to summertime melting and warming (Gordon et al., 1977). The entrainment of upper circumpolar deep water (UCDW) into the T_{min} layer continues while the surface layer above it remains isolated. Thus, the T_{min} layer represents a long-term mixing zone between the summer surface layer and the UCDW (Smith and Treguer, 1994). In this case, the N_2O produced under the T_{min} layer should diffuse into it and then either be transported or escape into the atmosphere via sea-air exchange. Thus, we can estimate the inventory of excess N_2O by assuming that N_2O from the UCDW source is transported to the upper layer by simple diffusion. Assuming a vertical eddy-diffusion coefficient of 0.6 cm^2 s^{-1} (Li et al., 1984) and the measured gradients of ΔN_2O between N_2O maxima to the lower T_{min} layer, these calculations yield an upward N_2O flux of 0.041 to 0.048 μmol m^{-2} d^{-1}, with an average of 0.045 μmol m^{-2} d^{-1} which in the range of those observed by Law and Ling (2001), and we obtain the isotopomeric signature of $\delta^{15}N^{bulk}$ = 13.2‰, $\delta^{18}O$ = 51.8‰, and a site preference of 7.3‰ for the source.

BGD
7, 7821–7848, 2010

Information about the distribution of N_2O in other areas of the Southern Ocean is lacking. Therefore, as noted above, the influence of Southern Ocean N_2O on the global N_2O budget cannot be calculated. A conservative estimate shows that the N_2O flux determined in this study would produce about 46.2 ± 5.3 Mg N_2O-N d^{-1}. This value is based on the assumption of upward N_2O flux and a total surface area of the Southern Ocean of 37×10^{12} m^2 (Peng, 1984). This low production rate may be due to the simultaneous production and consumption of N_2O. However, this upward N_2O flux from the N_2O maxima layer can be diluted or transferred by the current of fresh water from melted ice. Thus, N_2O emission may occur in other areas depending upon the flow and diffusion rates. Furthermore, the existing data suggest that the area around the Southern Ocean is a large N_2O sink. We can estimate the dynamic exchange rate of N_2O to be about -3.76 ± 2.67 Gg N_2O-N d^{-1} using the sea-air flux and N_2O diffusion from the N_2O maximum layer calculation.

5 Conclusions

The horizontal and vertical distributions of dissolved N_2O in the Southern Ocean during the austral summer show characteristic features related to the production of phytoplankton and zooplankton, which are most abundant during this season. Furthermore, the characteristics of the various water masses in the Southern Ocean may also be governed by the production and removal of dissolved N_2O. In this study, the following important facts should be emphasized:

The concentration and isotopic composition of dissolved N_2O in the surface water are suggested to be associated with the transfer velocity around the Southern Ocean. Surface N_2O is at about 94% saturation and the calculated dynamic sea-air flux is on average -3.68 µmol m^{-2} d^{-1}. This negative value can be explained by physical factors and the marine movement from the glacial region.

BGD
7, 7821–7848, 2010

The vertical distributions of N_2O display a maximum layer around 150–300 m (ΔN_2O, 7.90–8.51 nM) and coincide with the oxygen minimum layer. The N_2O maximum layer occurs below the chlorophyll-*a* maximum layer, suggesting a relationship between N_2O production and consumption and plankton dynamics in this area. N_2O production derives from aerobic and/or semi-anaerobic conditions, depending upon the redox boundaries by using the isotopic viewpoints.

In the deeper layer, the existence of anoxic microsites within particles, together with the horizontal and vertical movements of cold water from inshore, induced by the geopotential anomaly of the strong steering current of the ridge system around the Antarctic, are parameters that control the isotopic composition of N_2O, at least in part.

The influence of Southern Ocean N_2O on the global N_2O budget was estimated to be about -3.76 ± 2.67 Gg N_2O-N d^{-1}, based on the sea-air flux and the assumption of upward N_2O flux caused by diffusion from the maximum layer to the T_{min} layer.

Acknowledgements. We acknowledge funding from the Japan Science and Technology Agency (JST). We would like to thank Wada E. and an anonymous reviewer, who commented constructively on the manuscript. We also thank the officers and crew members of the R/V *Tangaroa* for their cooperation.

References

Alldredge, A. L. and Cohen, Y.: Can microscale chemical patches persist in the sea? Microelectrode study of marine snow, fecal pellets, Science, 235, 689–691, 1987.

Bieri, R. H., Koide, M., and Goldberg, E. D.: The noble gas contents of Pacific sea waters, J. Geophys. Res., 71, 5243–5265, 1966.

Bieri, R. H., Koide, M., and Goldberg, E. D.: Noble gas contents of marine waters, Earth Planet. Sci. Lett., 4, 329–333, 1968.

Boontanon, N., Ueda, S., Kanatharana, P., and Wada, E.: Intramolecular stable isotope ratios of N_2O in the tropical swamp forest in Thailand, Naturwissenschaften, 87, 188–192, 2000.

Bouwman, A. L.: Exchange of greenhouse gases between terrestrial ecosystems and the at-

BGD
7, 7821–7848, 2010

mosphere, in: Soil and greenhouse effect, edited by: Bouwman, A. L., John Wiley & Sons, New York, 61–127, 1990.
Broecker, H. C. and Siems, W.: The role of bubbles for gas transfer from water to air at higher windspeeds. Experiments in the wind-wave facility in Hamburg, in: Gas transfer at water surfaces, edited by: Brutsaert, W. and Jirka, G. H., D. Reidel Pub. Co., Dordrecht, 229–236, 1994.
Butler, J. H., Elkins, J. W., and Thompson, T. M.: Tropospheric and dissolved N_2O of the west Pacific and east Indian Oceans during El Niño Southern Oscillation event of 1987, J. Geophys. Res., 94, 14865–14877, 1989.
Central Intelligence Agency (CIA): The world factbook: Southern Ocean, available at: http://www.cia.gov/cia/publications/factbook/geos/oo.html, 2003.
Cohen, Y. and Gordon, L. I.: Nitrous oxide in the oxygen minimum of the eastern tropical North Pacific: Evidence for its consumption during denitrification and possible mechanisms for its production, Deep-Sea Res., 25, 509–524, 1978.
Cohen, Y. and Gordon, L. I.: Nitrous oxide production in the ocean, J. Geophys. Res., 84, 347–353, 1979.
Crutzen, P. J.: The influence of nitrogen oxides on the atmospheric ozone content, Q. J. Roy. Meteorol. Soc., 96, 320–325, 1970.
Dore, J. E., Popp, B. N., Karl, D. M., and Sansone, F. J.: A large source of atmospheric nitrous oxide from subtropical North Pacific surface water, Nature, 396, 63–66, 1998.
Elkins, J. W., Wofsy, S. C., McElroy, M. B., Kolb, C. E., and Kaplan, W. A.: Aquatic sources and sinks for nitrous oxide, Nature, 275, 602–606, 1978.
Gordon, A. L., Georgi, D. T., and Taylor, H. W.: Antarctic Polar Front zone in the western Scotia Sea-Summer 1975, J. Phys. Oceanogr., 7, 309–328, 1977.
Hirawake, T., Kudoh, S., Aoki, S., and Rintoul, S. R.: Eddies revealed by SeaWiFS ocean color images in the Antarctic Divergence zone near 140° E, Geophys. Res. Lett., 30, 1458, doi:10.1029/2003GL016996, 2003.
Inoue, H. Y. and Mook, W. G.: Equilibrium and kinetic nitrogen and oxygen isotope fractionations between dissolved gaseous N_2O, Chem. Geol., 113, 135–148, 1994.
Kaplan, W. A. and Wofsy, S. C.: The biogeochemistry of nitrous oxide: A review, in: Advances in aquatic microbiology, edited by: Jannasch, H. W. and Williams, P. J. B., Academic Press, Florida, 181–206, 1985.
Kim, K. R. and Craig, H.: Nitrogen-15 and oxygen-18 characteristics of nitrous oxide: A global

BGD
7, 7821–7848, 2010

perspective, Science, 262, 1855–1857, 1993.
Knowles, R., Lean, D. R. S., and Chan, Y. K.: Nitrous oxide concentrations in lakes: Variations with depth and time, Limnol. Oceanogr., 26, 855–866, 1981.
Law, C. S. and Ling, R. D.: Nitrous oxide flux and response to increased iron availability in the Antarctic Circumpolar Current, Deep-Sea Res. Pt. II, 48, 2509–2527, 2001.
Li, Y. H., Peng, T. H., Broecker, W. S., and Östlund, H. G.: The average vertical mixing coefficient for the oceanic thermocline, Tellus B, 36, 212–217, 1984.
Liss, P. S. and Slater, P. G.: Flux of gases across the air-sea interface, Nature, 247, 181–184, 1974.
Lutjeharms, J. R. E.: The oceanography and fish distribution of the Southern Ocean, in: Fishes of the Southern Ocean, edited by: Gon, O. and Heemstra, P. C., Smith J. L. B. Institute of Ichthyology, Grahamstown, 6–27, 1990.
Naqvi, S. W. A., Jayakumar, D. A., Nair, M., Kumar, M. D., and George, M. D.: Nitrous oxide in the western Bay of Bengal, Mar. Chem., 47, 269–278, 1994.
Naqvi, S. W. A., Yoshinari, T., Jayakumar, D. A., Altabet, M. A., Narvekar, P. V., Devol, A. H., Brandes, J. A., and Codispoti, L. A.: Budgetary and biogeochemical implications of N_2O isotope signatures in the Arabian Sea, Nature, 394, 462–464, 1998.
Oris, A. H., Whitworth III, M., and Nowlin Jr., W. D.: On the meridional extent and fronts of the Antarctic Circumpolar Current, Deep-Sea Res. Pt. I, 42, 641–673, 1995.
Ostrom, N. E., Russ, M. E., Popp, B. N., Rust, T. M., and Karl, D. M.: Mechanisms of nitrous oxide production in the subtropical North Pacific based on determinations of the isotopic abundances of nitrous oxide and di-oxygen, Chemosphere Global Change Sci., 2, 281–290, 2000.
Peng, T. H.: Invasion of fossil fuel CO_2 into the ocean, in: Gas transfer at water surfaces, edited by: Brutsaert, W. and Jirka, G. H., D. Reidel Pub. Co., Dordrecht, 589–595, 1984.
Popp, B. N., Westley. M. B., Toyoda, S., Miwa, T., Dore, E., Yoshida, N., Rust, T. M., Sansone, F. J., Russ M. E., Ostrom, N. E., and Ostrom, P.: Nitrogen and oxygen isotopomeric constraints on the origins and sea-to-air flux of N_2O in the oligotrophic subtropical North Pacific gyre, Global Biogeochem. Cycles, 16, 1064, doi:10.1029/2001GB001806, 2002.
Rysgaard, S., Risgaard-Petersen, N., Nielsen, L. P., and Revsbech, N. P.: Nitrification and denitrification in lake and estuarine sediments measured by the ^{15}N dilution technique and isotope pairing, Appl. Environ. Microb., 59, 2093–2098, 1993.
Schmidt, H. L. and Voerkelius, S.: Origin and isotope effects of oxygen in compounds of the

BGD
7, 7821–7848, 2010

nitrogen cycle, in: Proceedings of 5th working meeting on isotopes in nature, Leipzig, 613–624, 1989.
Sigman, D. M., Altabet, M. A., McCorkle, D. C., Francois, R., and Fischer, G.: The δ^{15}N of nitrate in the Southern Ocean: Consumption of nitrate in surface waters, Global Biogeochem. Cycles, 13, 1149–1166, 1999.
Smith, N. and Treguer, P.: Physical and chemical oceanography in the vicinity of Prydz Bay, Antarctica, in: Southern Ocean ecology: the BIOMASS perspective, edited by: El-Sayed, S. Z., Cambridge University Press, New York, 25–43, 1994.
Svensson, J. M.: Emission of N_2O, nitrification and denitrification in a eutrophic lake sediment bioturbated by *Chironomus plumosus*, Aquat. Microb. Ecol., 14, 289–299, 1998.
Toyoda, S. and Yoshida, N.: Determination of nitrogen isotopomers of nitrous oxide on a modified isotope ratio mass spectrometer, Anal. Chem., 71, 4711–4718, 1999.
Toyoda, S., Yoshida, N., Miwa, T., Matsui, Y., Yamagishi, H., Tsunogai, U., Nojiri, Y., and Tsurushima, N.: Production mechanism and global budget of N_2O inferred from its isotopomers in the western North Pacific, Geophys. Res. Lett., 29, 1037, doi:10.1029/2001GL014311, 2002.
Ueda, S., Ogura, N., and Yoshinari, T.: Accumulation of nitrous oxide in aerobic ground water, Water Res., 27, 1787–1792, 1993.
Ueda, S., Yoshioka, T., Go, C. S. U., Wada, E., Khodzher, T., Gorbunova, L., Zhdanov, A., Igor, K., Bashenkhaeva, N., and Tomberg, I.: Nitrogen and oxygen isotope ratios of N_2O in Lake Baikal, in: Response of Land Ecosystems to Global Environmental Changes, edited by: Wada, E., Kyoto University, Kyoto, 28–35, 1999.
Wada, E., Terazaki, M., Kabaya, Y., and Nemoto, T.: ^{15}N and ^{13}C abundances in the Antarctic Ocean with the emphasis on the biogeochemical structure of the food web, Deep-Sea Res., 34, 829–841, 1987.
Wada, E., Yoshida, N., Yoshioka, T., Yoh, M., and Kabaya, Y.: The abundance of ^{15}N in N_2O in aquatic ecosystems with emphasis on denitrification, Mitt. Internat. Verein. Limnol., 25, 115–123, 1996.
Wahlen, M. and Yoshinari, T.: Oxygen isotope ratios in N_2O from different environments, Nature, 313, 780–782, 1985.
Watson, R. T., Meira Filho, L. G., Sanhueza, E., and Janetos, T.: Sources and sinks, in: Climate Change 1992, edited by: Houghton, J. T., Callander, B. A., and Varney, S. K., Cambridge University Press, Cambridge, 25–46, 1992.

BGD
7, 7821–7848, 2010

Weeg-Aerssens, E., Tiedje, J. M., and Averill, A.: Evidence from isotope labeling studies for a sequential mechanism for dissimilatory nitrite reduction, J. Am. Chem. Soc., 110, 6851–6856, 1988.
Weiss, R. E. and Price, B. A.: Nitrous oxide solubility in water and seawater, Mar. Chem. 8, 347–359, 1980.
Yoshida, N.: Nitrogen isotope studies on the geochemical cycle of nitrous oxide, Ph.D. thesis, Tokyo Institute of Technology, Tokyo, Japan, 192 pp., 1984.
Yoshida, N.: ^{15}N-depleted N_2O as a product of nitrification, Nature, 335, 528–529, 1988.
Yoshida, T. and Alexander, M.: Nitrous oxide formation by *Nitrosomonas europaea* and heterotrophic microorganisms, Soil Sci. Soc. Am. Pro., 34, 880–882, 1970.
Yoshida, N., Morimoto, H., Hirano, M., Koike, I., Matsuo, S., Wada, E., Saino, T., and Hattori, A.: Nitrification rates and ^{15}N abundances of N_2O and NO_3^- in the western North Pacific, Nature, 342, 895–897, 1989.
Yoshida, N. and Toyoda, S.: Constraining the atmospheric N_2O budget from intramolecular site preference in N_2O isotopomers, Nature, 405, 330–334, 2000.
Yoshinari, T.: Nitrous oxide in the sea, Ph.D. thesis, Dalhousie University, Nova Scotia, Canada, 112 pp., 1973.
Yoshinari, T.: Nitrous oxide in the sea, Mar. Chem., 4, 189–202, 1976.

BGD
7, 7821–7848, 2010

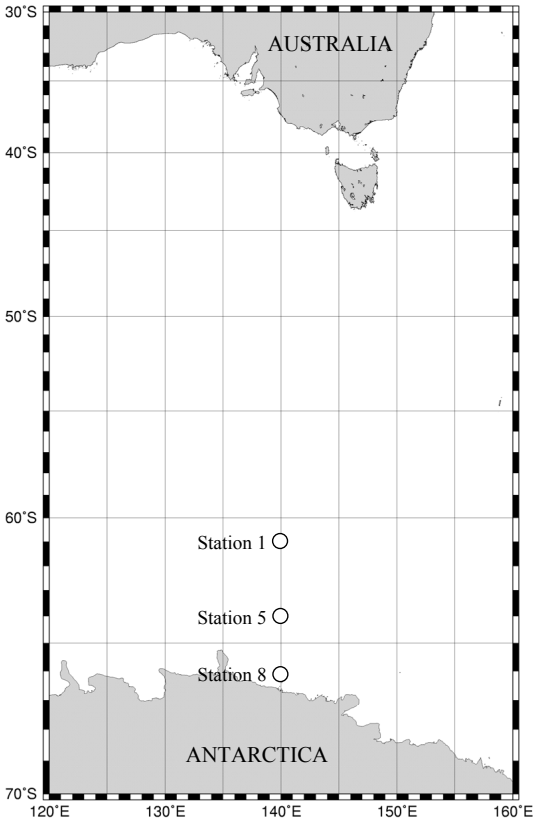

Fig. 1. Location of sampling stations during the JARE-43 Marine Science Cruise on the R/V *Tangaroa*.

BGD
7, 7821–7848, 2010

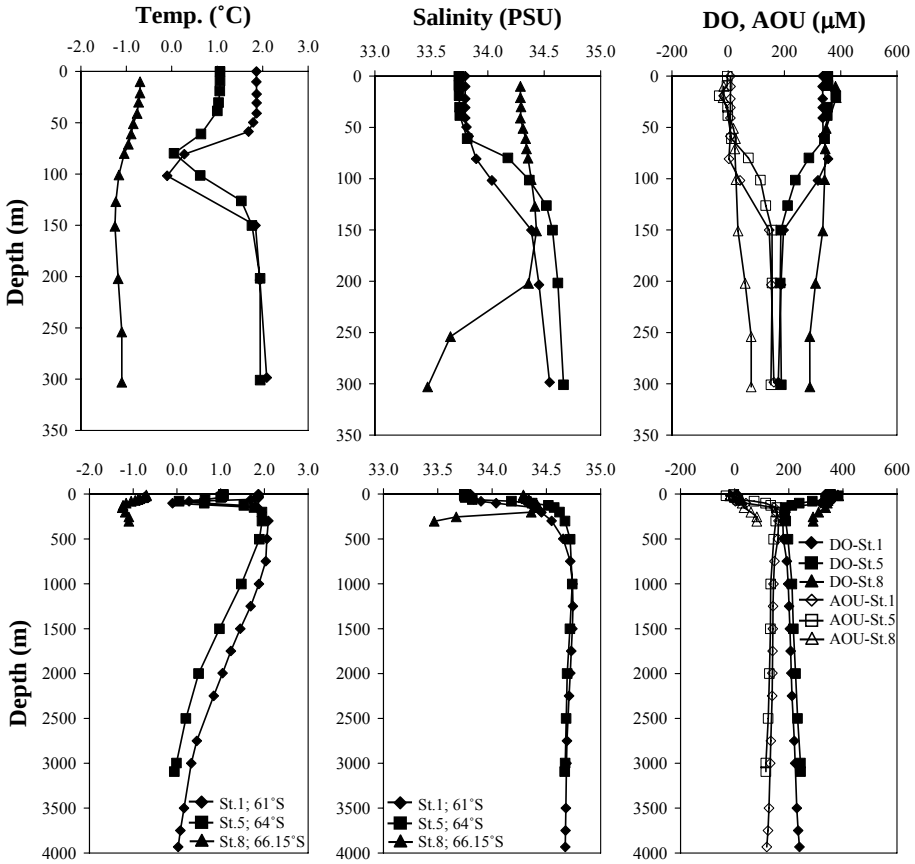

Fig. 2. Vertical profiles at 140˚ E for temperature, salinity, dissolved oxygen, and apparent oxygen utilization. Top row highlights the upper 350 m.

BGD
7, 7821–7848, 2010

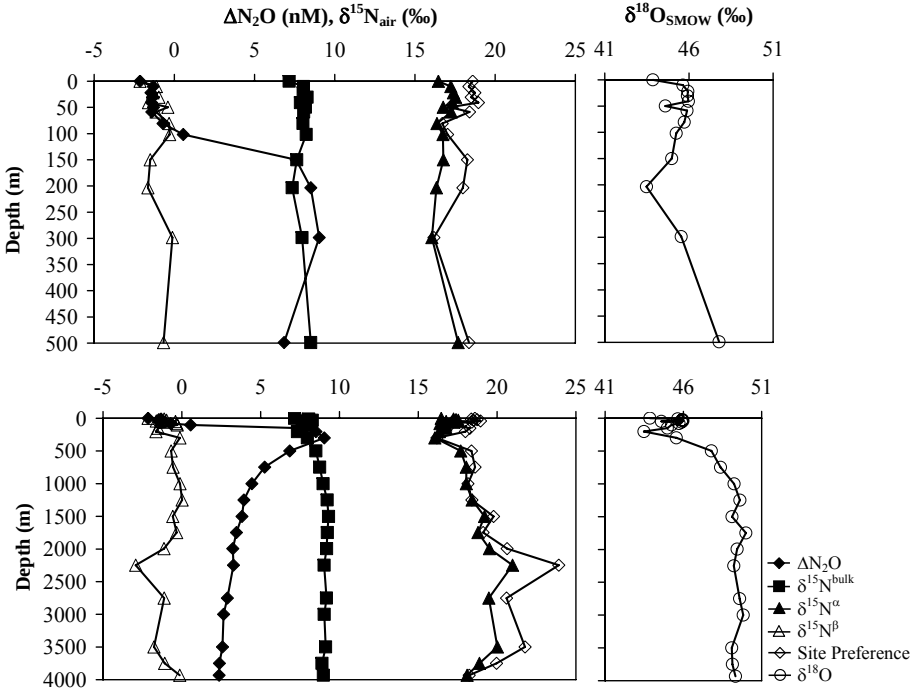

Fig. 3. Vertical profiles of excess N_2O, isotopomer ratios ($\delta^{15}N^{bulk}$, $\delta^{15}N^{\alpha}$, $\delta^{15}N^{\beta}$, and $\delta^{18}O$), and ^{15}N site preference ($\delta^{15}N^{\alpha} - \delta^{15}N^{\beta}$) of N_2O observed at station 1 (61° S). Top row highlights the upper 500 m.

BGD
7, 7821–7848, 2010

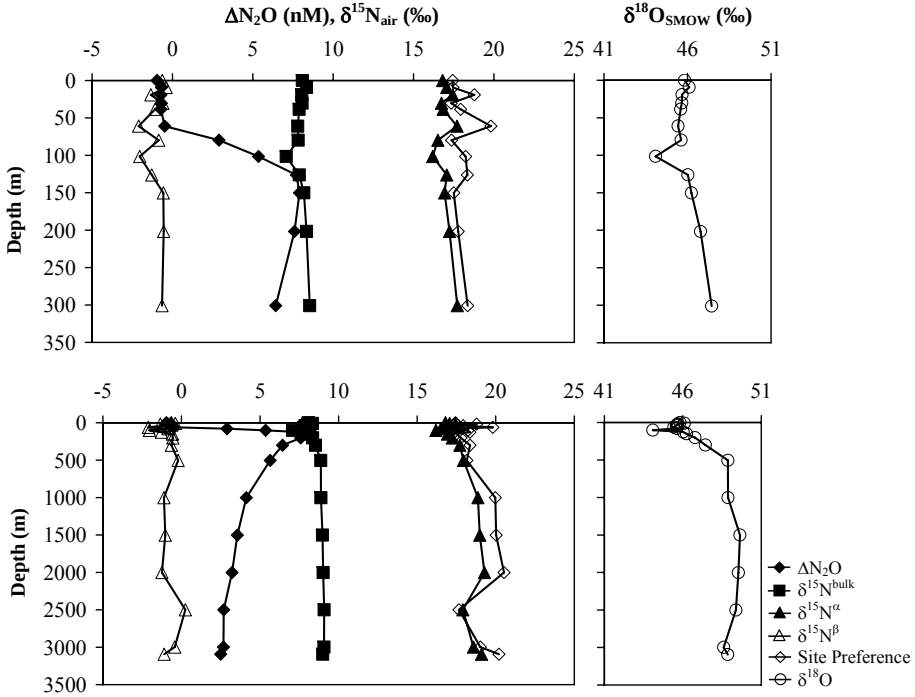

Fig. 4. Vertical profiles of excess N_2O, isotopomer ratios ($\delta^{15}N^{bulk}$, $\delta^{15}N^{\alpha}$, $\delta^{15}N^{\beta}$, and $\delta^{18}O$) and ^{15}N site preference ($\delta^{15}N^{\alpha} - \delta^{15}N^{\beta}$) of N_2O observed at station 5 (64° S). Top row highlights the upper 350 m.

BGD
7, 7821–7848, 2010

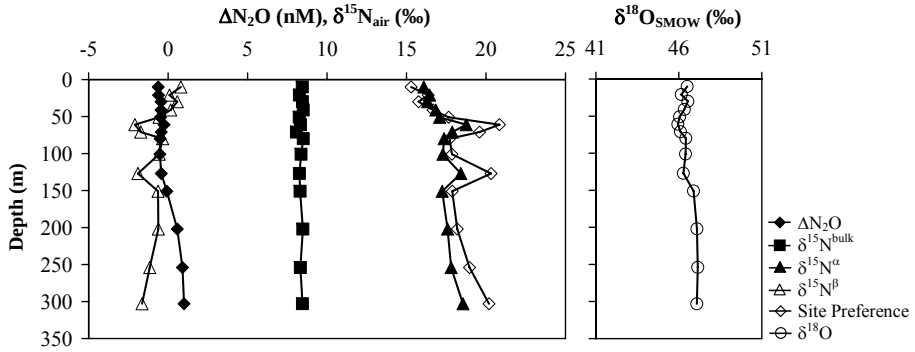

Fig. 5. Vertical profiles of excess N_2O, isotopomer ratios ($\delta^{15}N^{bulk}$, $\delta^{15}N^{\alpha}$, $\delta^{15}N^{\beta}$, and $\delta^{18}O$), and ^{15}N site preference ($\delta^{15}N^{\alpha} - \delta^{15}N^{\beta}$) of N_2O observed at station 8 (66.15° S).

BGD
7, 7821–7848, 2010

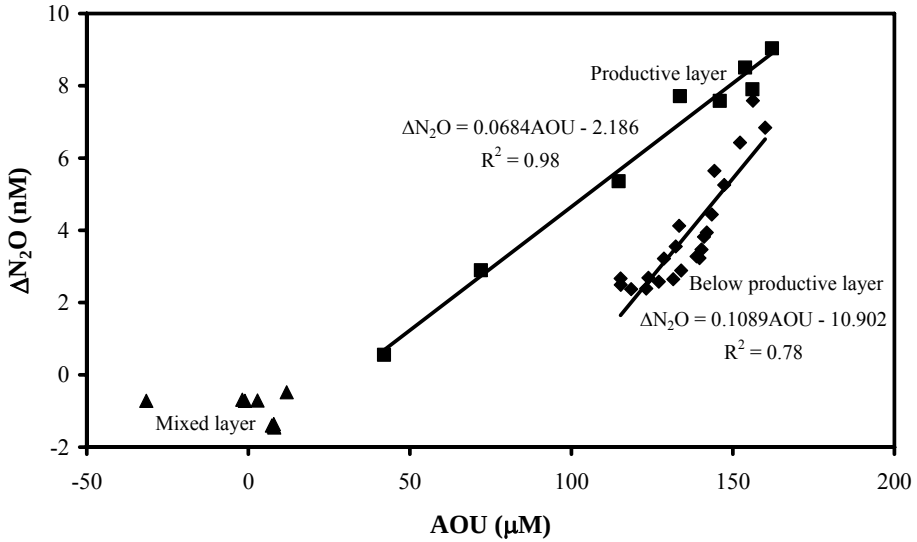

Fig. 6. Correlation of ΔN_2O and AOU at stations 1 and 5. ΔN_2O in the mixed layer, below mixed layer to maximum layer, and below maximum layer plotted as triangles, squares, and diamonds, respectively.

BGD
7, 7821–7848, 2010

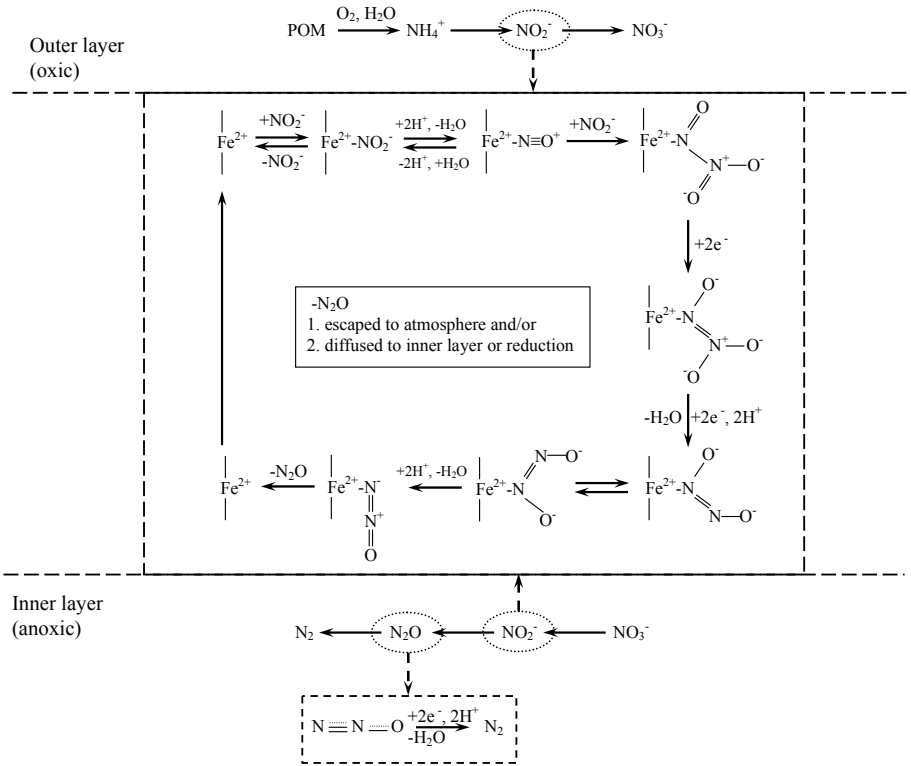

Fig. 7. Proposed pathways for the formation and destruction of N_2O from the reduction of nitrite. The involvement of enzyme-bond intermediates is shown (modified from Weeg-Aerssens et al., 1988).

BGD
7, 7821–7848, 2010

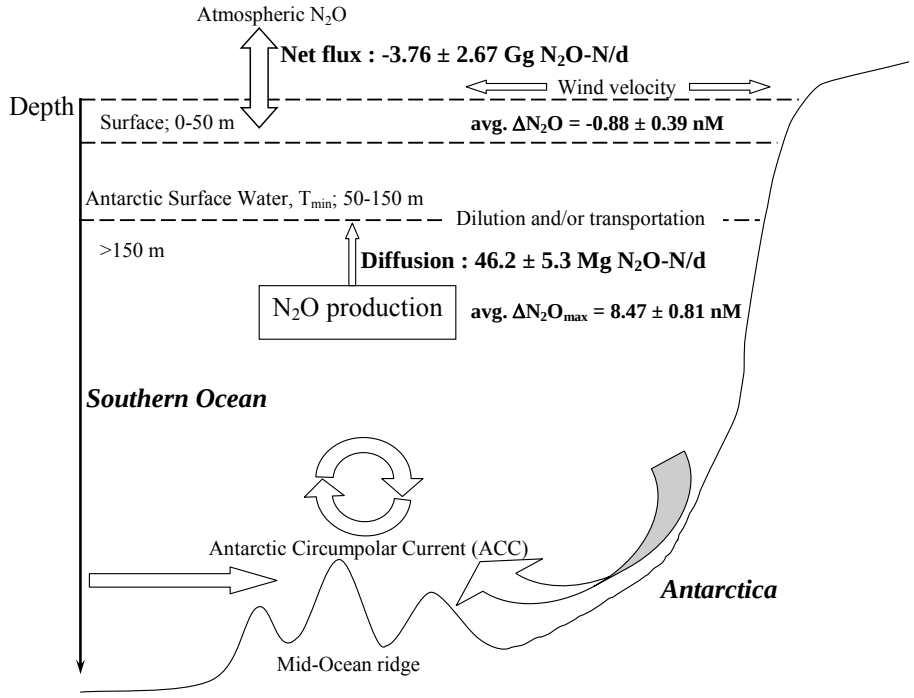

Fig. 8. Summary of the effects of dissolved N_2O in the Southern Ocean.

BGD
7, 7821–7848, 2010